Supporting Information

Biomimetic Oxygen-Evolving Photobacteria Based on Amino Acid and Porphyrin Hierarchical Self-Organization

Kai Liu[†,§], Han Zhang,[†] Ruirui Xing,[†] Qianli Zou,[†] and Xuehai Yan[*,†,‡,§]

[†]State Key Laboratory of Biochemical Engineering, Institute of Process Engineering, Chinese Academy of Sciences, 100190 Beijing, China

[‡]Center for Mesoscience, Institute of Process Engineering, Chinese Academy of Sciences, 100190 Beijing, China

[§]University of Chinese Academy of Sciences, 100190 Beijing, China

Homepage: http://www.yan-assembly.org

Email: yanxh@ipe.ac.cn

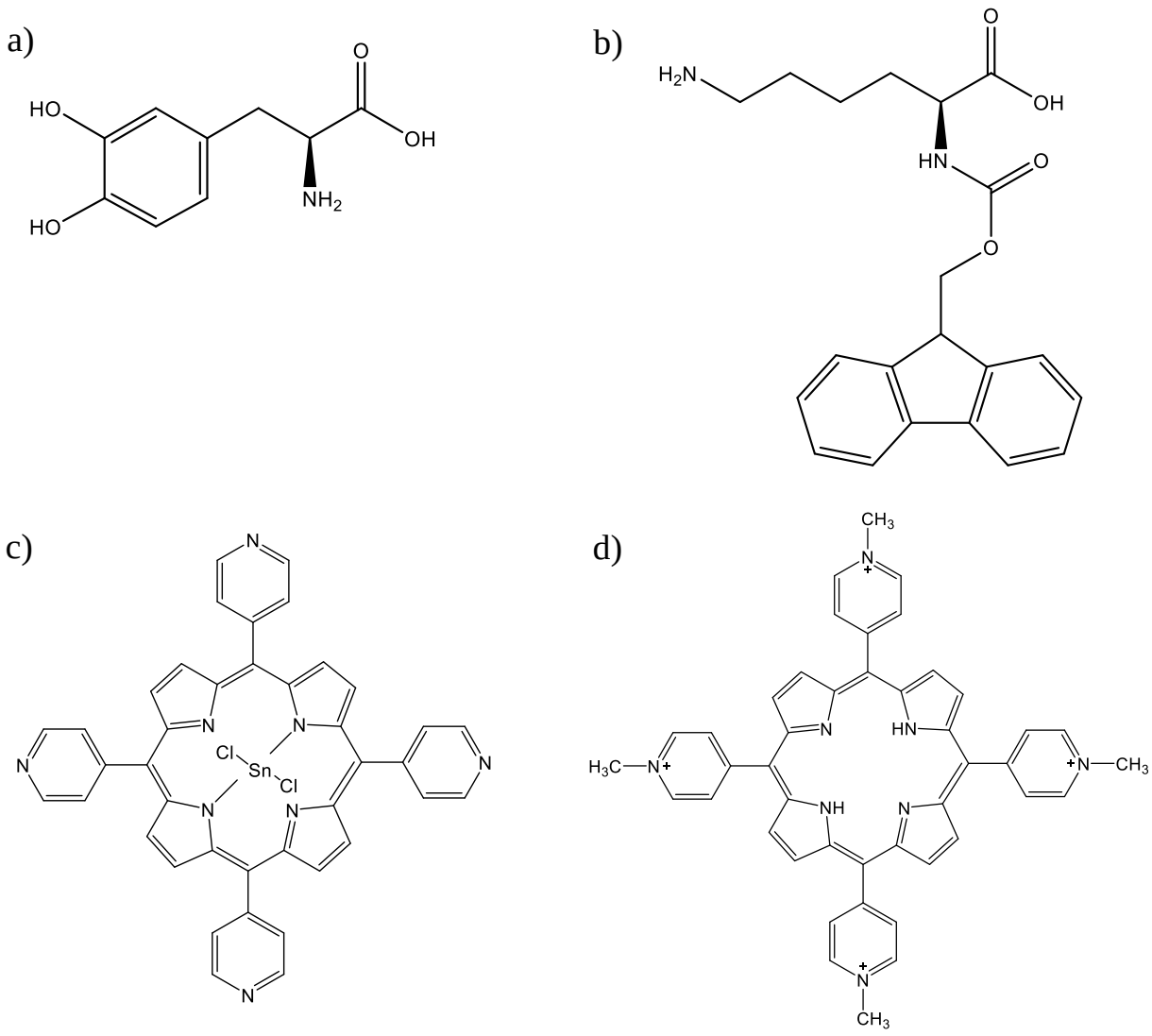

Figure S1. Molecular structures of (a) L-3,4-dihydroxyphenylalanine (L-DOPA), (b) 9-Fluorenylmethoxycarbonyl-L-lysine (Fmoc-L-Lys), (c) Sn(IV) tetrakis(4-pyridyl)porphyrin ($SnTPyP^{2+}$), (d) Meso-Tetra(4-N-methylpyridyl)porphyrine ($TMPyP^{4+}$).

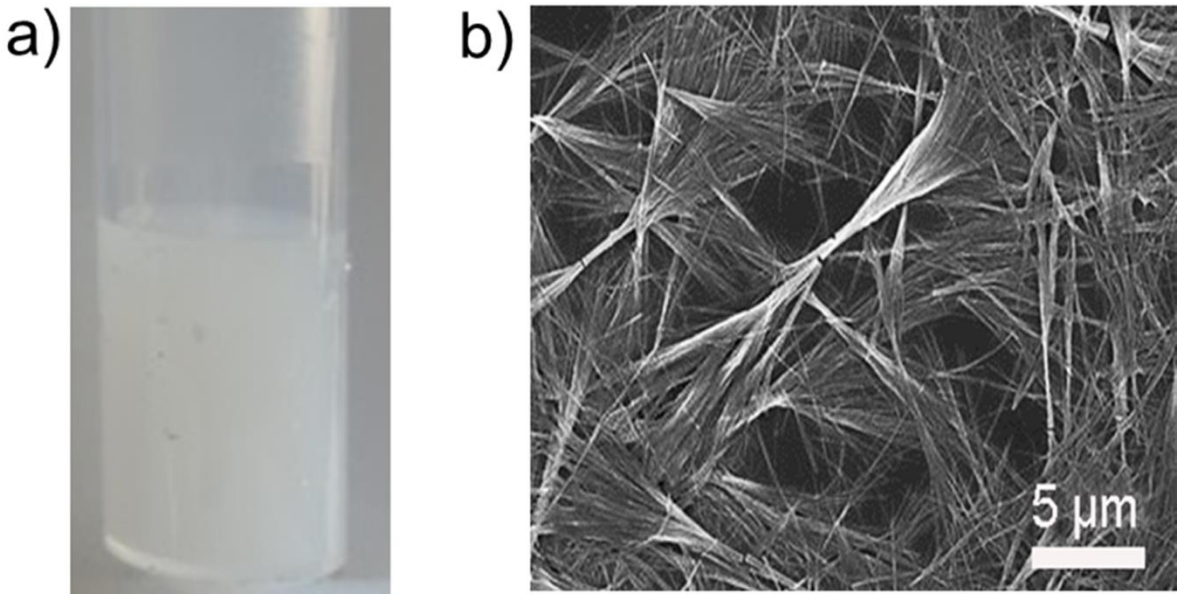

Figure S2. a) Photograph of an assembled Fmoc-L-Lys fiber solution, which is white and turbid. b) SEM image of assembled Fmoc-L-Lys fibers, showing solid fibrous structure.

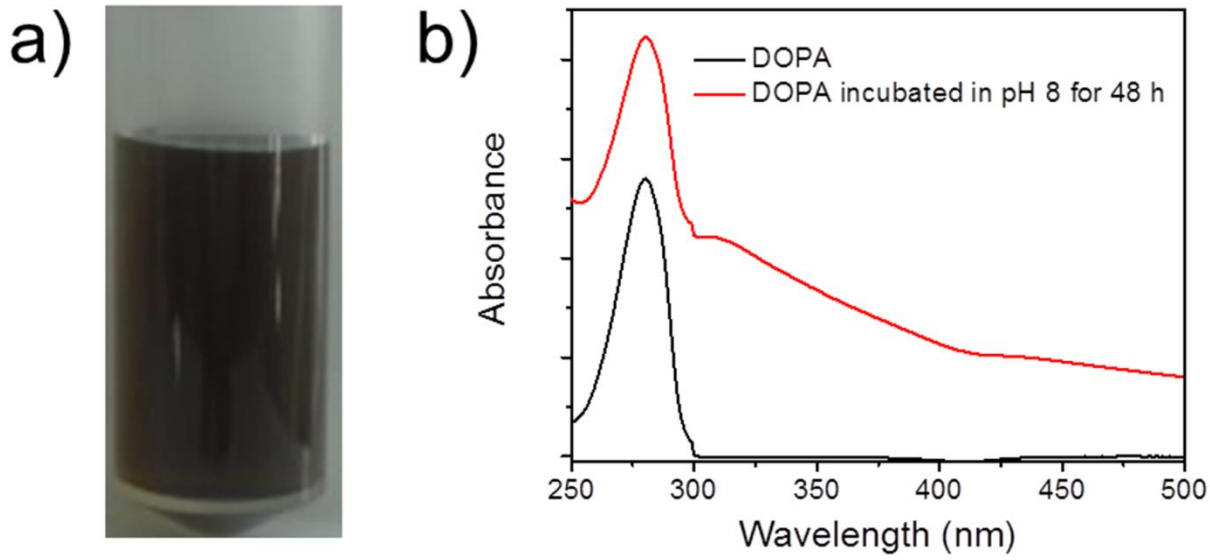

Figure S3. a) Photograph of DOPA (1 mg mL^{-1}) after incubation at pH 8 for 48 h. b) UV-vis absorption spectra of a DOPA (1 mg mL^{-1}) solution before and after incubation at pH 8 for 48h. The base line for the absorbance spectrum in the range of 300~500 nm has a varying elevation, showing the feature of DOPA melanin.[1]

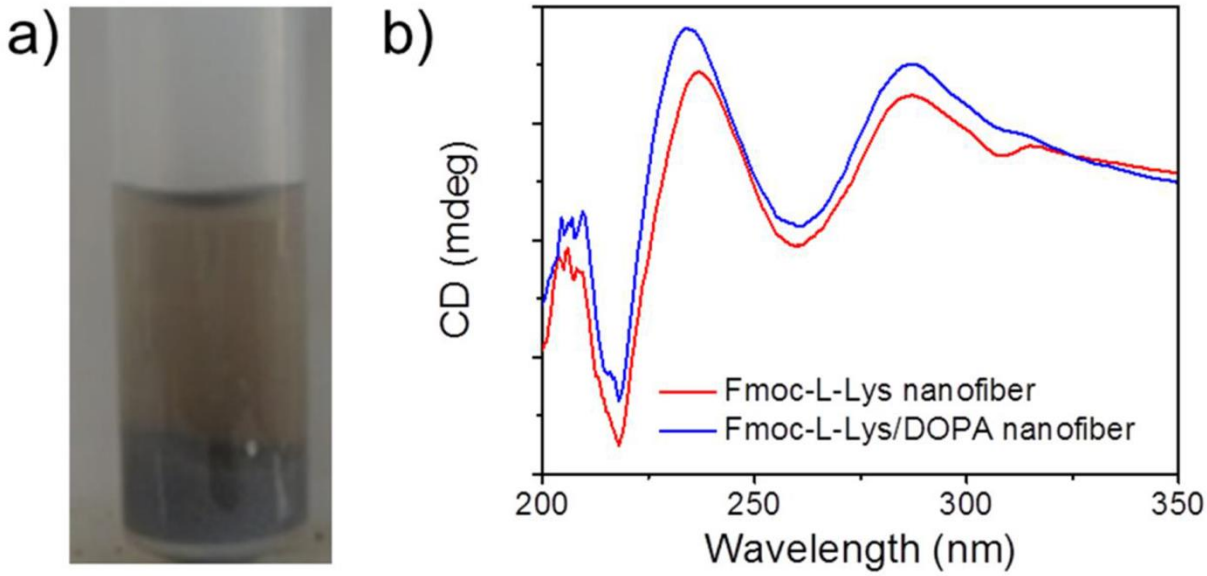

Figure S4. a) Photograph of Fmoc-L-Lys fibers after incubation with DOPA (1 mg mL^{-1}) at pH 8.0 for 2 days. c) CD spectra of Fmoc-L-Lys and Fmoc-L-Lys/DOPA fibers. They show similar peak patterns, indicating that the structures of assembled Fmoc-L-Lys are retained in Fmoc-L-Lys/DOPA fibers.

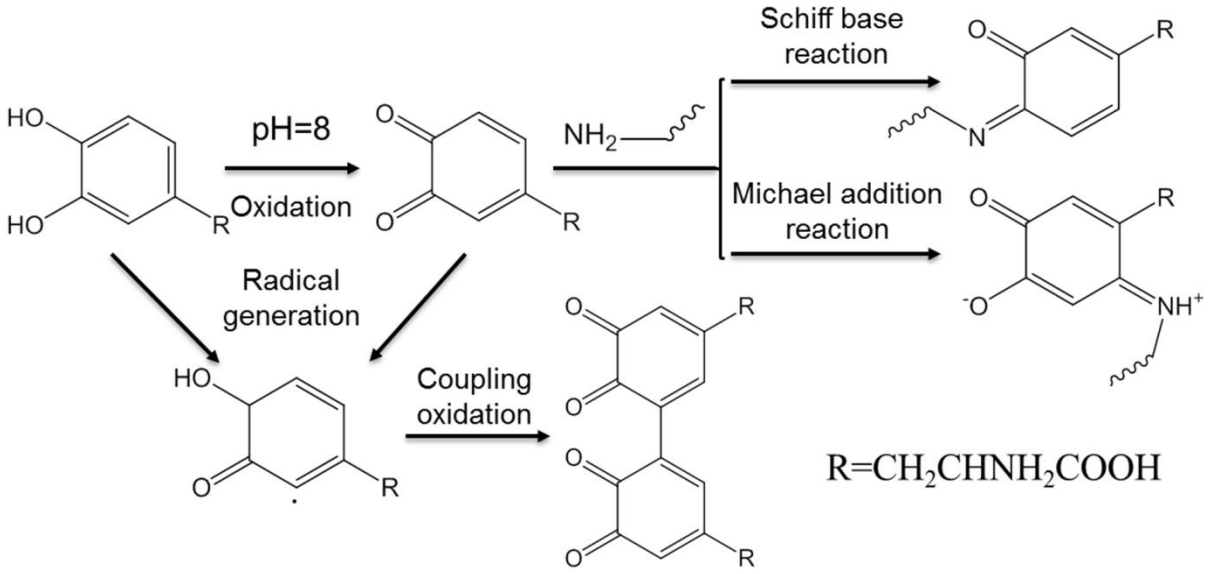

Figure S5. Possible oxidative and cross-linking reaction mechanism for DOPA. Autoxidation of DOPA is induced in alkaline pH and DOPAquinone is generated.[2,3] The quinone then couples to form bisquinone (or oligomers) units.[4] Quinone intermediate can be attacked by nucleophiles (e.g., amino group) *via* a Michael addition and/or Schiff base reaction.[3,5-8] Oxidation of DOPA followed by polymerization is the key step for the formation of DOPA melanin.[1]

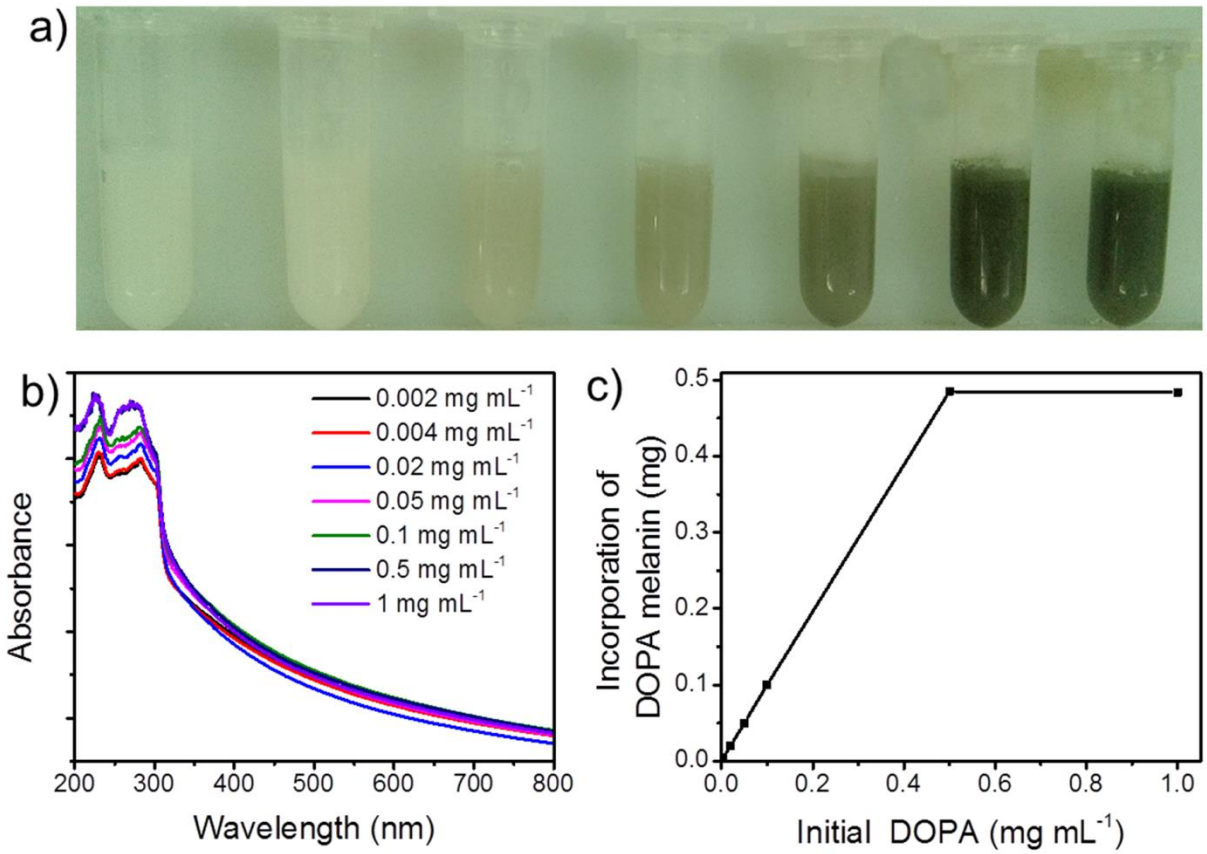

Figure S6. a) Photograph of Fmoc-L-Lys fibers (5 mg mL^{-1}) after incubation with different concentration of DOPA (from left to right: 2×10^{-3} mg mL^{-1}, 4×10^{-3} mg mL^{-1}, 2×10^{-2} mg mL^{-1}, 5×10^{-2} mg mL^{-1}, 1×10^{-1} mg mL^{-1}, 5×10^{-1} mg mL^{-1} and 1 mg mL^{-1}) at pH 8.0 for 2 days. Before analysis the finial precipitate was centrifuged at 4000 rpm for 10 min and resuspended in ultrapure water. b) UV-Vis absorption spectra of resulting Fmoc-L-Lys/DOPA fibers in (a). As the increase of initial concentration of DOPA, the according Fmoc-L-Lys/DOPA fibers have an increase absorbance at 280 nm ascribed to DOPA melanin. This absorbance reaches saturation when DOPA is given at 5×10^{-1} mg mL^{-1}. c) The amount of incorporated DOPA melanin at different initial concentration of DOPA. When the concentration of DOPA is lower than 5×10^{-1} mg mL^{-1}, the added DOPA can fully be incorporated into Fmoc-L-Lys fibers in form of DOPA melanin. 1 mL of Fmoc-L-Lys fibers (5mg mL^{-1}) has the capability to incorporate as much as 0.485 mg DOPA melanin.

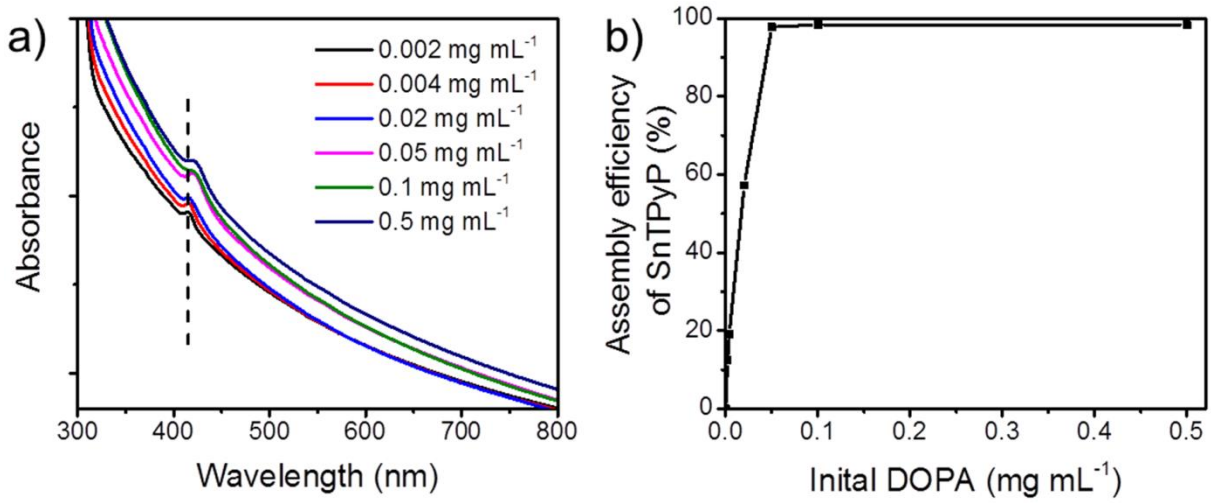

Figure S7. a) UV-Vis absorption spectra of Fmoc-L-Lys/DOPA/SnTPyP fibers at different concentration of DOPA. At low concentration of DOPA (2×10^{-3} mg mL^{-1}, 4×10^{-3} mg mL^{-1}, 2×10^{-2} mg mL^{-1}), the absorption peak is centered at 416 nm ascribed to SnTPyP monomer. When the concentration of DOPA reaches 5×10^{-2} mg mL^{-1}, the absorption peak red shifts to 423 nm, which is indicative of SnTPyP aggregate due to an increased amount of assembled SnTPyP. b) The assembly efficiency of SnTPyP (10 μM) on the Fmoc-L-Lys/DOPA fibers at different initial concentration of DOPA. The assembly efficiency of SnTPyP increases as the increase of DOPA concentration and reaches nearly 100 % when DOPA concentration is (or above) 5×10^{-2} mg mL^{-1}.

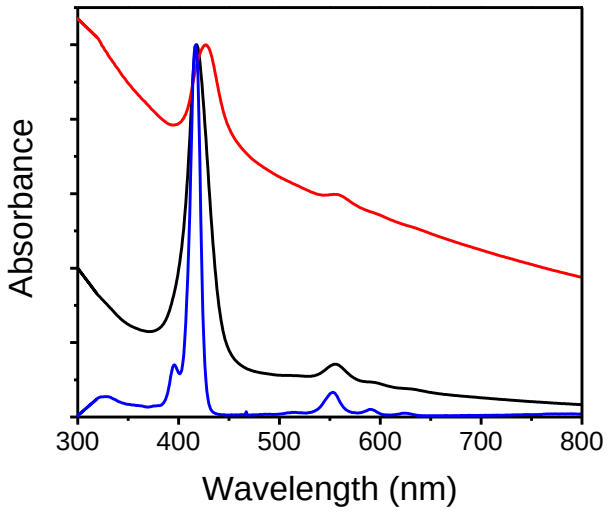

Figure S8. Normalized UV-Vis absorption spectra of SnTPyP (pre-dissolved in 1M HCl, blue line), SnTPyP mixed with DOPA melanin (black line) and Fmoc-L-Lys/DOPA/SnTPyP fibers (red line) in ultrapure water of pH 8.0 adjusted by 1 M NaOH. After incubation with DOPA melanin, the Sort band of SnTPyP becomes broader along with a little red shift. These changes are due to the coupling of DOPA melanin and SnTPyP, probably *via* coordination bond and electrostatic interaction. The Sort band of SnTPyP on the Fmoc-L-Lys/DOPA fibers further broadens and shows an obvious red shift. This is because the SnTPyP molecules in the fibers have a close distance, which facilitates the according intermolecular coupling. These results prove the vital role of the Fmoc-L-Lys template to tune self-assembly of SnTPyP.

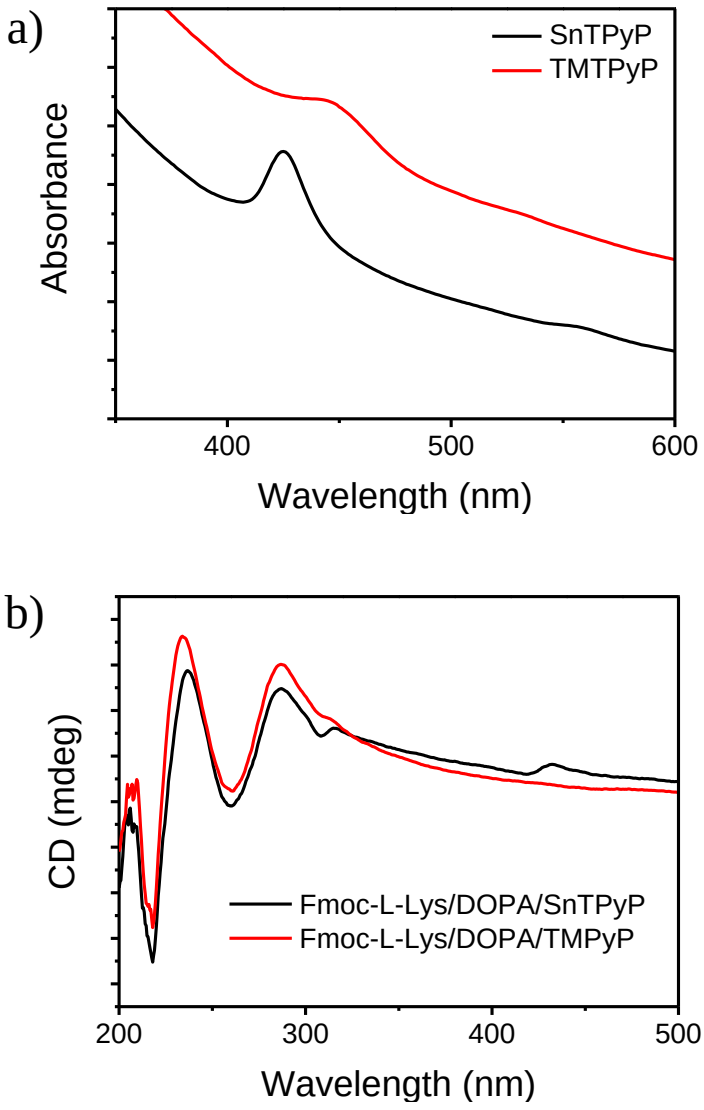

Figure S9. a) UV-Vis absorption spectra b) CD spectra of Fmoc-L-Lys/DOPA/SnTPyP Fmoc-L-Lys/DOPA/TMTPyP fibers in solution. TMTPyP and SnTPyP are both positively charged and have similar molecular structure. To investigate the effects of Sn center on the self-assembly of SnTPyP, we use TMTPyP as a control model without metal center. TMTPyP can be assembled onto the Fmoc-L-Lys/DOPA fibers *via* electrostatic interaction, however, the assembled TMTPyP molecules show no chiral signal. These results indicate, that the metal center in metalloporphyrin is indispensable for the ordered origination on the Fmoc-L-Lys/DOPA fibers.

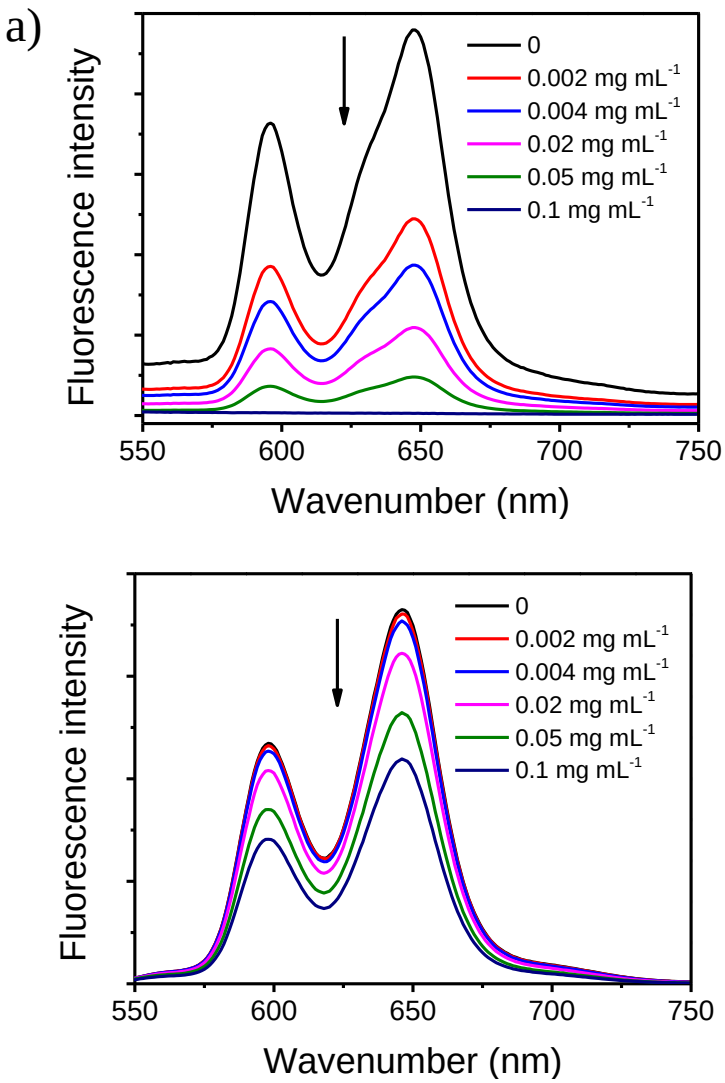

Figure S10. Fluorescence spectra of a) SnTPyP after mixing with DOPA melanin and b) Fmoc-L-Lys/DOPA/SnTPyP fibers in solution at different concentration of initial DOPA.

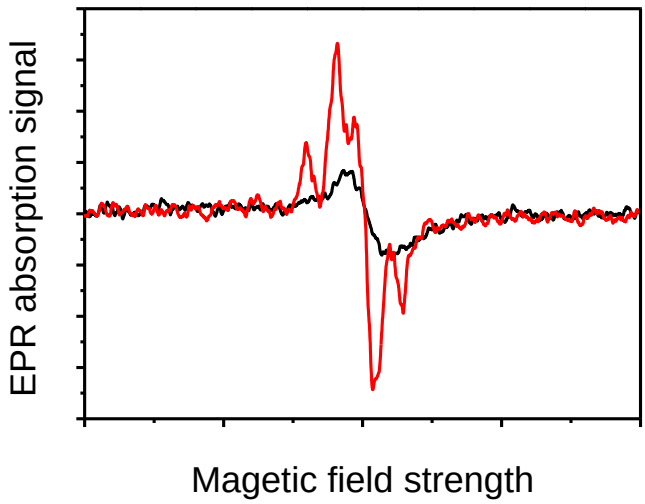

Figure S11. EPR spectra of DOPA after mixing of ammonia water (red line) and Fmoc-L-Lys/DOPA/SnTPyP fibers after illumination (black line). In basic condition, DOPA generates an intense EPR signal with a g value of 2.00194, which is derived from the overlap of a more dominant carbon-centered signal and the small semiquinone signal.[9] While the EPR signal from Fmoc-L-Lys/DOPA/SnTPyP fibers is weak and has a g value (2.00215) different to that of the former. This is probably because the electron transfer from light-excited SnTPyP to quinone and the generated semiquinone constitutes the main EPR signal.

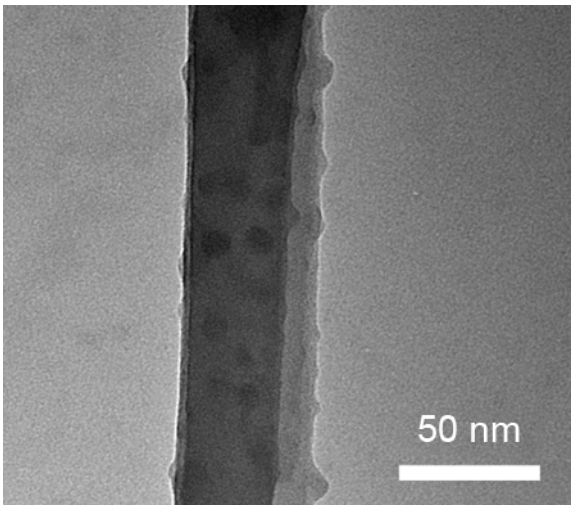

Figure S12. TEM image of Fmoc-L-Lys/DOPA/Co_3O_4 fibers. The Co_3O_4 NPs are inset on the surface of the fibers.

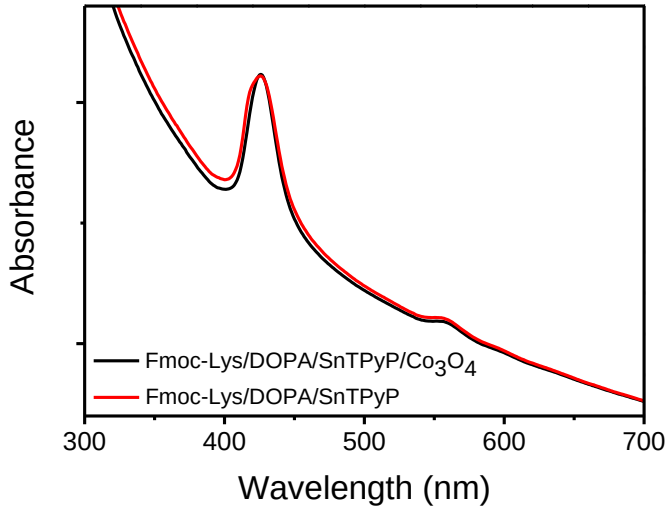

Figure S13. UV-Vis absorption spectra of Fmoc-L-Lys/DOPA/SnTPyP and Fmoc-L-Lys/DOPA/SnTPyP/Co_3O_4 hybrid fibers in solution.

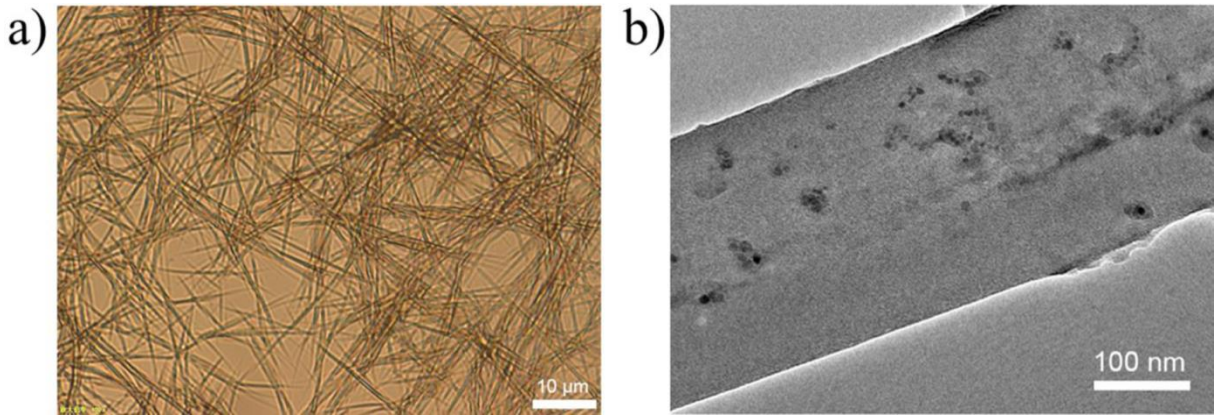

Figure S14. a) Optical and b) TEM images of Fmoc-L-Lys/DOPA/SnTPyP/Co_3O_4 hybrid fibers after constant stirring at 600 rpm for 6 h. The fibrous structure is observed after the stirring as before (Figure 1a), suggesting that the β-sheet structure based on π-stacking and H-bond is stable enough to resist mechanical agitation. The attached Co_3O_4 NPs remained during the constant stirring indicative of the robustness of the hybrid fibers. Co_3O_4 NPs can attach on the assembled fibers *via* coordination binding, although the adhesive interaction may become weaker considering the alkaline condition. The electronic attraction between the positively charged nanoparticles and the negatively charged carboxyl groups in the fibers can also enhance the binding.

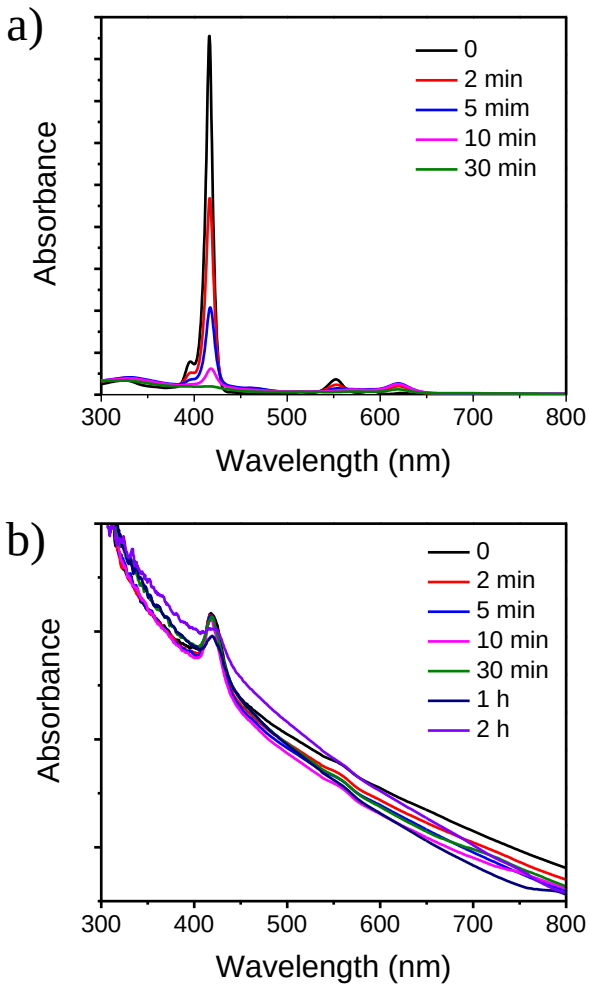

Figure S15. UV-Vis absorption spectra of a) SnTPyP and b) Fmoc-L-Lys/DOPA/SnTPyP in borate buffer solution (pH 8.0, 10 mM) containing sodium persulfate (5 mM) after irradiation under visible light ($\lambda \geqslant 400$ nm) for different period of time. The mixed solutions were exposed to air condition and stirred at a speed of 600 rpm. The Soret band of free SnTPyP quickly declines and disappears after 30 min irradiation, resulting from the photobleaching of SnTPyP probably *via* oxidation by single oxygen or sodium persulfate. After 30 min irradiation the Soret band of Fmoc-L-Lys/DOPA/SnTPyP is almost unchanged and can remain ca. 40% intensity after 2 h irradiation. This enhanced photostability for Fmoc-L-Lys/DOPA/SnTPyP is probably due to exciton migration among J-aggregated SnTPyP.

Reference

(1) Panzella L.; Gentile G.; D'Errico G.; Della Vecchia N. F.; Errico M. E.; Napolitano A.; Carfagna C.; d'Ischia M. Atypical Structural and π-Electron Features of a Melanin Polymer That Lead to Superior Free-Radical-Scavenging Properties. *Angew. Chem. Int. Ed.* **2013**, *52*, 12684-12687.

(2) Wei, W.; Yu, J.; Broomell, C.; Israelachvili, J. N.; Waite, J. H., Hydrophobic Enhancement of Dopa-Mediated Adhesion in a Mussel Foot Protein. *J. Am. Chem. Soc.* **2012**, *135*, 377-383.

(3) Utzig T.; Stock P.; Valtiner M. Resolving Non-Specific and Specific Adhesive Interactions of Catechols at Solid/Liquid Interfaces at the Molecular Scale. *Angew. Chem. Int. Ed.* **2016**, *128*, 9676-9680.

(4) Yu M.; Hwang J.; Deming T. J. Role of L-3, 4-dihydroxyphenylalanine in Mussel Adhesive Proteins. *J. Am. Chem. Soc.***1999**, *121*, 5825-5826.

(5) Burzio, L. A.; Waite, J. H., Cross-Linking in Adhesive Quinoproteins: Studies with Model Decapeptides. *Biochemistry* 2000, *39*, 11147-11153.

(6) Burdine, L.; Gillette, T. G.; Lin, H.-J.; Kodadek, T., Periodate-Triggered Cross-Linking of Dopa-Containing Peptide-Protein Complexes. *J. Am. Chem. Soc.* **2004**, *126*, 11442-11443.

(7) Lee H.; Scherer N. F.; Messersmith P. B. Single-Molecule Mechanics of Mussel Adhesion. *Proc. Natl. Acad. Sci. U. S. A.* **2006**, *103*, 12999-13003.

(8) Tian, Y.; Cao, Y.; Wang, Y.; Yang, W.; Feng, J., Realizing Ultrahigh Modulus and High Strength of Macroscopic Graphene Oxide Papers through Crosslinking of Mussel-Inspired Polymers. *Adv. Mater.* **2013**, *25*, 2980-2983.

(9) Mostert A. B.; Hanson G. R.; Sarna T.; Gentle I. R.; Powell B. J.; Meredith P. Hydration-Controlled X-band EPR Spectroscopy: A Tool for Unravelling the Complexities of

the Solid-State Free Radical in Eumelanin. *J. Phys. Chem. B* **2013**, *117*, 4965-4972.